Activation energy of thermal fixing in $LiNbO_3$: a comparative study

M. A. Ellabban[a], G. Mandula[b], R. A. Rupp[a], M. Fally[a],
E. Hartmann[b], L. Kovács[b], K. Polgár[b]

[a]Institut für Experimentalphysik, Universität Wien,
Strudlhofgasse 4, A-1090 Wien, Austria.
[b]Crystal Physics Laboratory, Research Institute for Solid State Physics and Optics,
Hungarian Academy of Sciences, H-1525 Budapest, P.O. Box 49, Hungary

ABSTRACT

The activation energy of thermal fixing is determined in congruent and nearly stoichiometric lithium niobate crystals doped with manganese or iron, respectively. Three different techniques were employed: two-wave mixing, holographic scattering and DC conductivity measurements. A comparison between the three techniques is made and the possible reasons for the discrepancy in the values of the activation energy are discussed. Holographic techniques have the advantage of being contactless methods by which problems coming from electrodes effects are ignored. The holographic scattering technique is much simpler than two-wave mixing technique and gives the same results at high density of the compensating ions. At low free ions concentration it is an idealy sensitive technique to detect the possible dependence of the compensation time constant on the spatial frequency and to determine the concentration of free ions that are responsible for thermal fixing.

Keywords: Holography, Optical data storage, Thermal fixing

1. INTRODUCTION

Photorefractive materials (PRM) are the best candidates for reversible holographic storage applications. Different techniques were proposed to avoid destruction of stored information during read-out. One of the most important techniques used to achieve erase-resistant holograms is thermal fixing which was discovered by Amodei and Staebler.[1] It is based on the transformation of the information stored in the electronic-charge distribution into an ionic charge pattern which is stable against any further illumination. To that purpose the crystal is heated during or after holographic recording. Thereby, thermally activated ions compensate the recorded electronic charge pattern. Then the crystal is cooled to room temperature and illuminated homogeneously. Accordingly, the electronic pattern is redistributed thus revealing an ionic charge pattern which is stable against illumination. Thermal fixing improves the storage time considerably and allows for recording of many holograms in the same area without significant loss in the stored information.[2,3] A lot of work has been done to identify the mobile ions which compensate the electronic pattern and to clarify the mechanism of thermal fixing in order to control the fixing and development processes.[4–10] In most cases protons are identified as the only mobile ion below 180°C.[5,11,12] The individual thermally activated processes follow an Arrhenius law and can be characterized by a particular activation energy and a pre-exponential factor.[12]

Only recently we introduced a novel technique to determine the activation energy of thermal fixing in photorefractive crystals based on holographic scattering.[13] The occurrence of holographic scattering (HS) is a serious drawback that limits the applicability of thick recording media, but can favorably be exploited for material characterization.[14–17] It is much simpler than two-wave mixing (TWM) which is considered as one of the standard techniques for the determination of the activation energy for thermal fixing, particularly for long-time experiments with a high demand of vibration isolation. While in TWM a single grating characterized by a unique grating vector **K** is recorded, our technique monitors a signal generated by a distribution of **K**-vectors. The latter fact strongly resembles the typical situation of data storage applications where a host of gratings is stored in the PRM. Thus the results of HS experiments give quantities which are representative averages with respect to **K**. In the present work,

Further author information: (Send correspondence to R.A. Rupp) E-mail: Romano.Rupp@exp.univie.ac.at
M. A. Ellabban.: on leave from Tanta University, Egypt

we compare three different techniques which can be used to determine the activation energy of thermal fixing: HS and TWM which are contactless methods in determining the conductivity and standard DC-conductivity measurements (DCC). Four different types of lithium niobate crystals were investigated. Possible reasons for the slightly differing values of the activation energy determined by the different techniques are discussed.

2. EXPERIMENT AND RESULTS

Five lithium niobate samples from four types of crystals (Table 1) were investigated. Congruent and nearly stoichiometric $LiNbO_3$ crystals were grown by the Czochralski and the top-seeded solution growth methods, respectively. The crystals are doped with 1×10^{-3} mol/mol Mn or Fe.

Sample notation	Melt composition	Li/Nb	Dopant	$a \times b \times c$ [mm^3]
CMn	Congruent	0.945	Mn	$5.10 \times 4.35 \times 3.75$
SMn	Quasi-stoichiometric	0.99	Mn	$5.15 \times 3.60 \times 4.20$
CFe	Congruent	0.945	Fe	$4.85 \times 4.10 \times 3.75$
SFe1	Quasi-stoichiometric	0.99	Fe	$5.99 \times 3.96 \times 4.88$
SFe2	Quasi-stoichiometric	0.99	Fe	$6.02 \times 0.98 \times 4.89$

Table 1. Description of the investigated samples.

The sample holder and the heater are placed in a vacuum chamber to have a uniform temperature distribution in the sample and to avoid optical deteriorations of the optical paths by heat convection.

2.1. HS technique

An extraordinarily polarized laser beam impinges perpendicularly onto the sample and generates parasitic holograms. The incident intensity was 0.55 W/cm^2, the beam diameter was approximately 3 mm. The recording wavelength is $\lambda = 488$ nm except for the sample SFe1 in which parasitic holograms were recorded at λ=632.8 nm.

Each series of our experiment was achieved as follows: As a first step the parasitic hologram is recorded at room temperature till the transmitted intensity reaches a steady state, i.e. until the transmission does not decrease anymore. Then the sample is heated to the respective fixing temperature in the dark. Next, a very low intensity (I $= 3 \times 10^{-5}$ W/cm^2) is used to monitor the time dependence of the transmitted intensity. This step of reconstructing the recorded parasitic hologram during the compensation of the electronic pattern by the mobile ions continues till a complete compensation is reached and the transmission saturates as shown in Fig. 1(a). Finally, the sample is annealed at a high temperature ($\geq$150^{o}C) in the presence of white light for about 45 minutes to redistribute both, the ions and the electrons. This procedure ensures having the same initial conditions for the run of another fixing temperature. This series is repeated for several fixing temperatures.

By using proper fitting equations to our experimental data, the compensation time constant can be determined. Different fitting equations can be employed to our experimental data which are based either on a model for holographic scattering or on the diffraction theory for thick gratings.[13] The compensation time constant τ is assumed to obey the Arrhenius law: $\tau = \tau_0 \exp(-E_a/k_B T)$, where τ_0 is a pre-exponential factor, k_B is the Boltzmann constant, E_a is the activation energy of the process of compensation, and T is the absolute temperature. The evaluated compensation time constants for several fixing temperatures are shown in Fig. 2(a) and Fig2(b) for CMn and CFe, respectively.

2.2. TWM technique

A grating with a period of about 2 μm was recorded at room temperature using two ordinarily polarized beams of wavelength 488 nm. The grating vector is parallel to the c axis of the crystal. The runs of our experiment were performed in the same way as for the HS technique: After recording the grating at room temperature, the crystal is heated to the required fixing temperature. Then, the time dependence of diffraction efficiency is monitored using a low intensity as shown in Fig.1(b). Finally, the sample is annealed at high temperature for a long time in the presence of white light to be prepared for the run of the next temperature. A fitting equation, based on the diffraction theory of thick gratings, can be used to determine the compensation time constant at different fixing temperatures. It is given by the formula $\eta = \sin^2[\nu \exp(-t/\tau)]$, where ν is regarded as a fitting parameter.

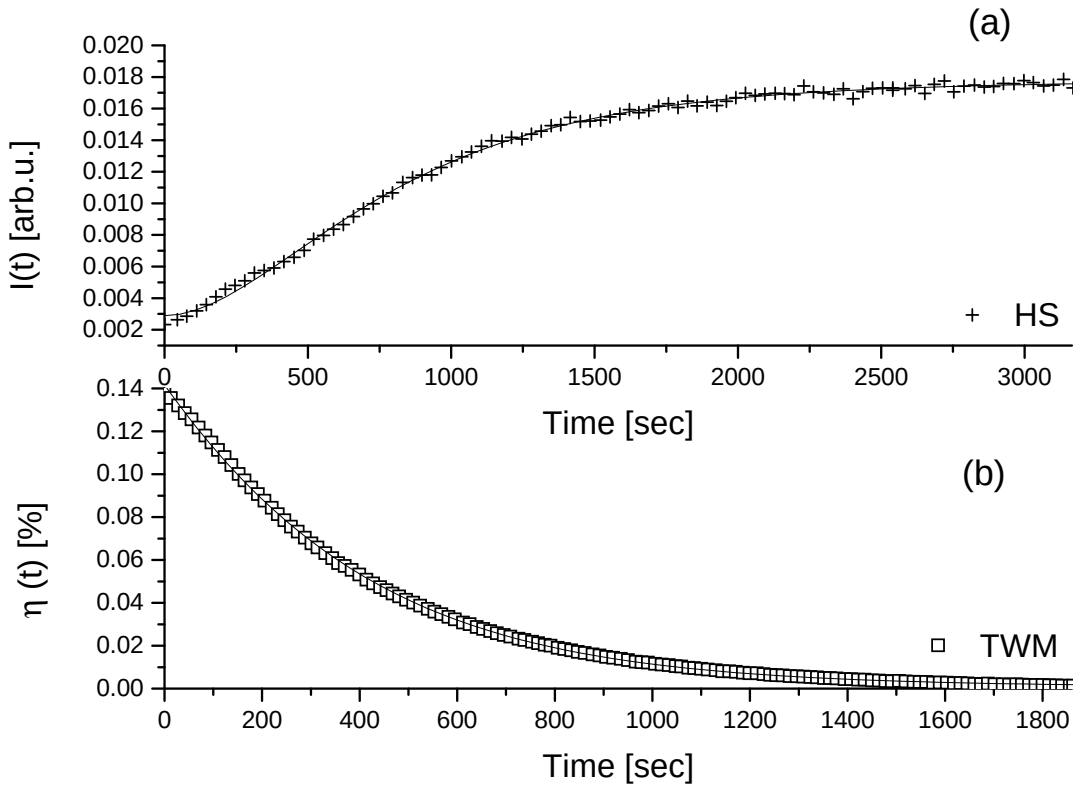

Figure 1. Time dependence of the transmitted intensity (HS method) and of the diffraction efficiency (TWM) due to compensation of the recorded (a) parasitic hologram and (b) conventional phase hologram at 100°C for the sample CMn. The solid lines represent fitting curves.

2.3. DCC technique

A DC-voltage of U=50 V was applied across the sample along the b direction, perpendicular to the polar axis, under vacuum of 3 Pa. The electrodes were made from silver paste. The current was measured as a function of temperature using a Keithley electrometer during cooling down of the sample with a rate of two degrees per minute. The Arrhenius plots for the calculated compensation time constant from the DCC measurements for CMn and CFe are shown in Fig.2(a) (open up triangles) and Fig.2(b) (open up triangles), respectively. The DC conductivity σ is related to the compensation time constant by the relation: $\sigma = \epsilon_0\epsilon/\tau$, where ϵ and ϵ_0 are the dielectric constant of the crystal and free space, respectively.

The values of the activation energy determined by the three different techniques are shown in Table 2. The error limits are calculated using the experimental and the statistical weighting methods. The major experimental error comes from the temperature measurements; the statistical errors of the fitting parameters are the minor errors. All these errors are considered in calculating the error limits.

3. DISCUSSION

Inspecting Table 2 it is striking that the results of the DCC deviate considerably from the values obtained by the other techniques, especially for the stoichiometric crystals. This may be due to the difference in the temperature range of the measurements with DCC and the holographic techniques[11,18]: The temperature range for DCC is 160-250 °C whereas it is 70-120 °C for the other methods.

Comparing the activation energy values determined from HS and TWM, only little deviation is found for the manganese doped samples whereas a significant deviation of 12 % is noted for the iron doped samples. In general,

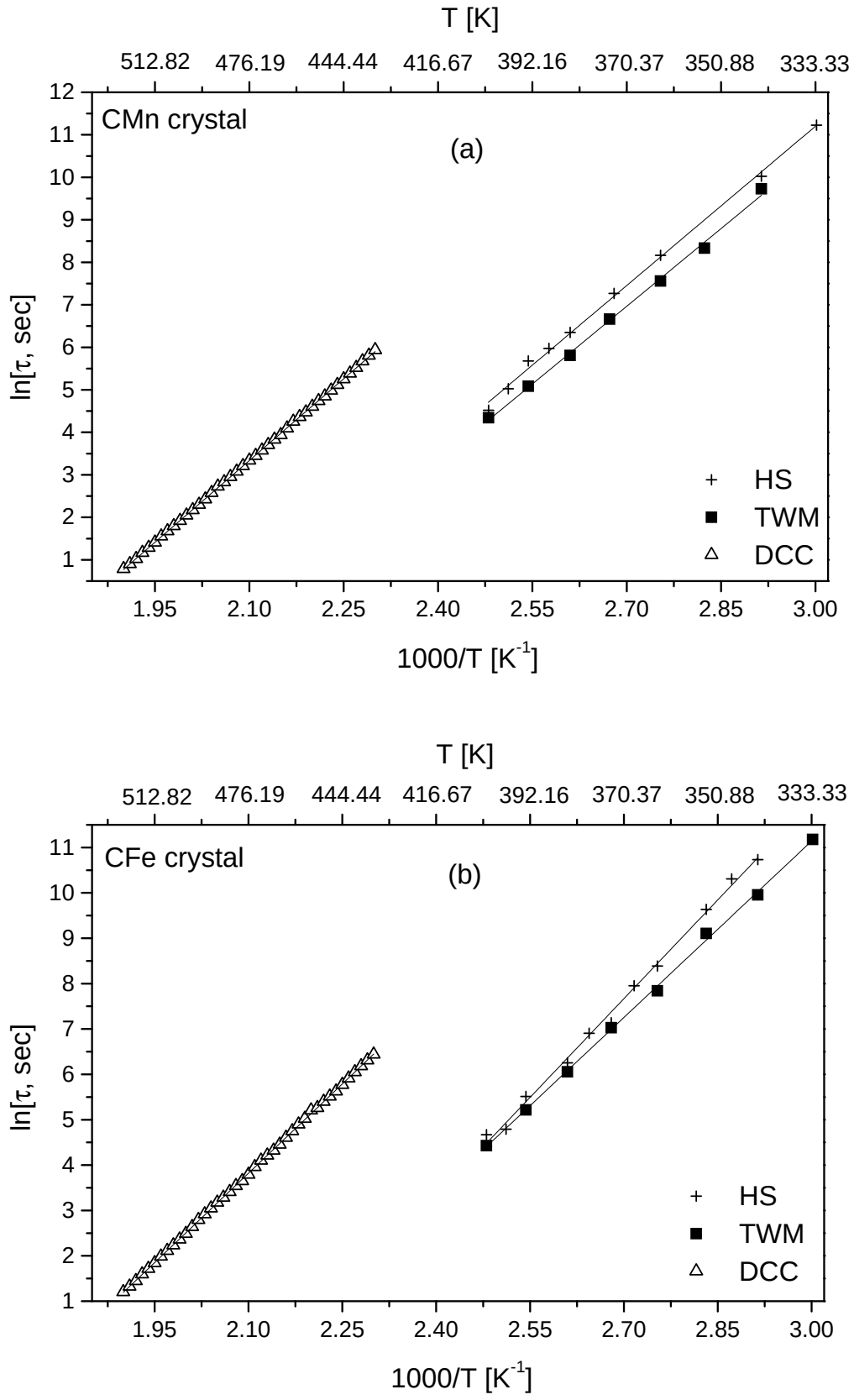

Figure 2. Arrhenius plot of the compensation time constant using HS (crosses), TWM (solid squares), and DCC (open up triangles) for (a) CMn crystal and (b) CFe crystal. The solid lines represent the fitting curves.

Sample	E_a (eV), HS	E_a (eV), TWM	E_a (eV), DC Conduct.
CMn	1.05 ± 0.03	1.06 ± 0.03	1.11 ± 0.03
SMn	1.05 ± 0.03	1.10 ± 0.03	0.96 ± 0.03
CFe	1.25 ± 0.03	1.12 ± 0.03	1.13 ± 0.03
SFe1	1.02± 0.04	-	0.95 ± 0.03
SFe2	-	1.10 ± 0.03	-

Table 2. Activation energy values determined using the three different techniques.

a certain discrepancy is noted between the values determined by the different techniques. What are the possible reasons for that discrepancy? We assume that they are related to the basic differences in both techniques. Here, we discuss two basic differences.

3.1. Spatial frequency of the recorded holograms

As said before, HS generates a multitude of **K**-vectors which differ from each other in both amplitude and direction whereas TWM creates a hologram with a unique **K**-vector. The thermally activated ions thus do not feel exactly the same structure in both cases. In the latter case they move in a periodic medium with one distinct K and in the first case in a complex medium structure with different Ks in TWM and HS, respectively. This means that we probe the relaxation time τ which is related to σ at different conditions (different **K** - vectors) when using the two different methods. This may be a reason for determining different values of E_a.

Additionally, the recording mechanism in $LiNbO_3$ is mainly driven by the local photovoltaic effect in addition to a nonlocal contribution generated by diffusion. The diffusion field E_D depends on $|\mathbf{K}|$= K according to the relation $E_D = K(k_BT/e)$ where e is the elementary charge. Therefore, it is not expected to have exactly the same situation in TWM and HS due the difference in **K**-vectors involved.

For those reasons let us calculate the influence of the spatial frequency K on τ. For simplicity we restrict the calculations to a single **K** - vector. The nonuniform illumination due to the interference between the pump and signal beam (during recording process at room temperature) excites electrons in the bright regions to migrate in the crystal and subsequently to be trapped at other sites (acceptors). The process of migration and trapping continues until the electrons migrate from the bright regions to the dark regions and an electronic charge density pattern $\rho_A(x) = \rho_A exp(iKx) + c.c.$ is created in the crystal. Next, the crystal is heated in dark to the required fixing temperature where the ions are assumed to be mobile. Let us assume in the following that the charge density of electrons trapped at acceptors due to the recording process does not depend on temperature.

The current density of the mobile ions,J_I, can be written as :

$$J_I = \sigma_I E - q_I D_I \frac{\partial N_I}{\partial x}, \tag{1}$$

where q_I is the ionic charge, D_I is the diffusion constant of the ions and E is the total electric field. The second term in Eq. 1 represents the diffusion current density. Inserting the current density and Poisson's equation $\epsilon_0\epsilon\partial E/\partial x = \rho_A + \rho_I$ in the continuity equation yields:

$$\frac{\partial \rho_I}{\partial t} + \frac{\rho_I}{\tau_I(K)} = -\frac{\rho_A}{\tau_{M,I} + KE_D\mu_I\rho_{I,0} + iKE_p\mu_I\rho_{I,0}}, \tag{2}$$

where

$$\tau_{M,I} = \frac{\epsilon_0\epsilon}{\sigma_{I,0}} \quad , \tag{3}$$

$$\tau_I(K) = \frac{\tau_{M,I}}{1 + \mu_I K(E_D + iE_p)\tau_{M,I}} \tag{4}$$

and E_p accounts for the photovoltaic field contribution.

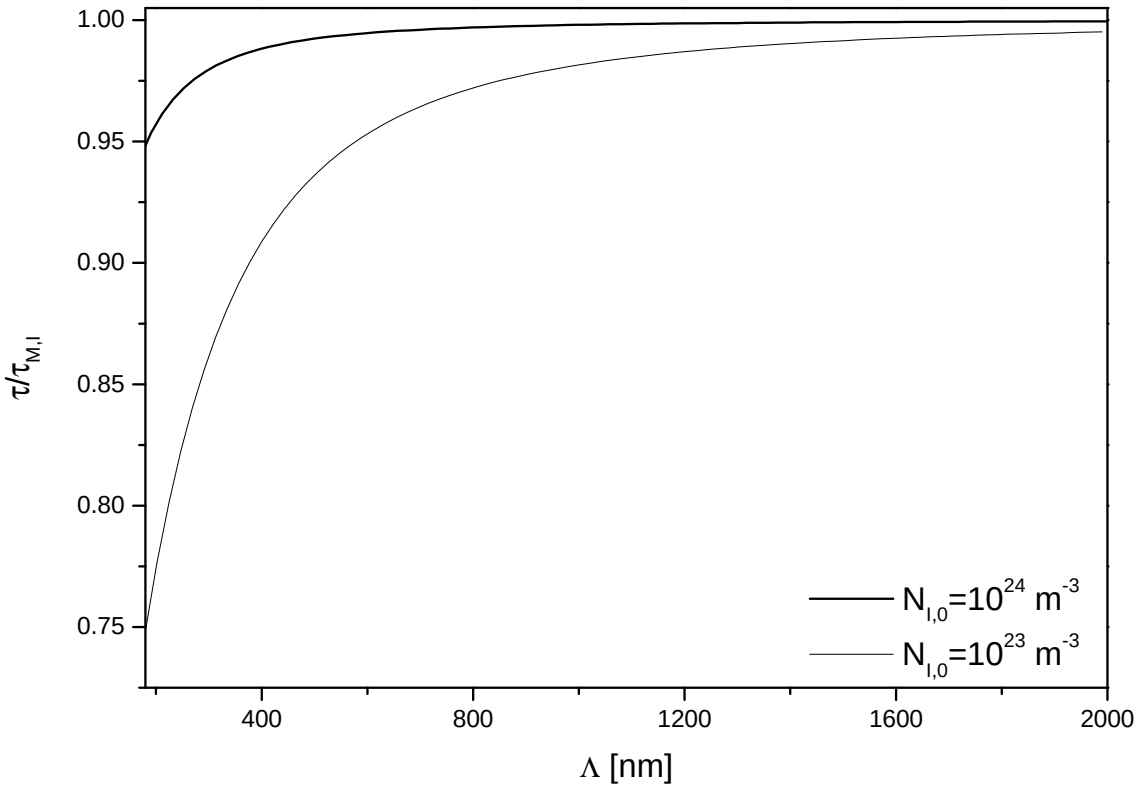

Figure 3. The grating period dependence of the ratio of the $\tau_I/\tau_{M,I}$ at two different ionic densities.

At steady state, Eq.2 and Eq.4 indicate that a complete compensation occurs only at $\tau_I(K=0) = \tau_{M,I}$. At K$\neq$ 0, the compensation is not complete because of thermal diffusion, thus $\rho_I < \rho_A$.

Equation 4 shows that the photovoltaic field will produce a phase shift (note the imaginary unity in front of E_p). The real part of $\tau_I(K)$ includes $E_D^2 + E_p^2$ in a term multiplied by a quadrate $(\epsilon\epsilon_0 K^2 k_B T/q_I N_{I,0})$. This quadrate is much less than unity in our crystals. Therefore, the whole term can be ignored and Eq.4 reduces to:

$$\tau_I(K) = \frac{\tau_{M,I}}{(1 + \epsilon\epsilon_0 K^2 k_B T/q_I^2 N_{I,0})} \tag{5}$$

The dependence of the compensation time constant on the spatial frequency is controlled through the term $\mu_I K E_D \tau_{M,I} = \epsilon\epsilon_0 K^2 k_B T/q_I^2 N_{I,0} = K^2 L_I^2$ with the diffusion length of the ions $L_I = (\sqrt{\epsilon\epsilon_0 k_B T/q_I^2 N_{I,0}})$. As long as this term is comparable to unity the effect of K must be taken into account. Using the known parameters of $LiNbO_3$ in literature[19,8] it can be seen from Eq.5 that the decisive quantity for the dependence of τ_I on K is the concentration of free ions $N_{I,0}$ in the crystal. Figure 3 shows the calculations of the ratio of $\tau_I(K)/\tau_{M,I}$ as a function of the grating period for two different values of the ion concentrations, $N_{I,0} = 1 \times 10^{23}$ and 1×10^{24} m^{-3}. At this point it might be thought that it is hopeless to detect the dependence of τ_I on K, but we should keep in mind that researchers always use the ion concentration determined from IR absorption spectra.[8] In fact this is the concentration of the **bound** ions whereas **free** ions are the only ions that are responsible for thermal fixing process. The ratio between the concentration of free and bound ions is not known and the assumption that it is equal to one is not always true. If the ratio is assumed to be less than one, the real dependence of τ_I on K is expected to be larger than the calculated one in Fig.3.

Equation 5 provides us with a valuable information provided that the dependence of τ_I on spatial frequency can be detected. It enables us, namely, to determine the density of **free** ions which are responsible for the thermal

fixing process. Staebler et al. and Yariv et al. found that the fixing time, ionic compensation, does not depend strongly on the spatial frequency.[3,20] This might be due to two reasons: The first is that they used crystals with high concentration of ions which shows a small dependence as expected from Eq.5. The second is the use of TWM technique which is not favorable for detecting the K dependence of τ_I. In TWM technique, the gratings should be recorded at first at a certain K, then the temperature is increased to the fixing temperature and the time dependence of the diffraction efficiency is measured. Finally one has to ensure having the same initial conditions for the next spatial frequency. As we are sometimes looking for a very small variation which requires having exactly the same initial conditions, any small deviation in the initial conditions will not help us to detect such small changes in τ_I. In fact it is difficult to use TWM in this situation (although it was done by Mu̇ller et al.[21]). On the other hand, HS produces a host of **K**-vectors which are recorded, heated to the fixing temperature and reconstructed in dark exactly at the same conditions. Thus, we propose HS to be the ideal technique for this purpose. If we can detect a change in the compensation time at different **K**-vectors, $N_{I,0}$ can be determined. This experiment is important and deserves our attempt. In fact, we need to determine the density of free ions once to know the ratio of the free ions and the bounded ions concentration for each photorefractive crystal. This can be used to calibrate the values determined from spectroscopic techniques.

According to Eq.5 at high $N_{I,0}$, the quantity τ_I does almost not depend on the spatial frequency. Under such conditions all recorded grating vectors in HS are compensated with the same time constant and HS technique can be expected to give the same results as TWM technique. At low $N_{I,0}$ and large K, according to Fig.3, the dependence of τ_I on K has to be taken into account.

3.2. The modulation depth [m(K)]

The second reason for the discrepancy in the values of activation energy when using HS and TWM may be the modulation m(K). Since HS originates from the interference between the pump beam and its scattered beams, HS has always a very low modulation, $m = 2\sqrt{(I_s I_p)}/(I_s + I_p)$, in comparison with TWM. The space charge field in the steady state can be written as $E(\mathbf{K}) = -E_{eff} m(K)$, where $m(K)$ is the modulation and E_{eff} is a complex quantity. If we considered that HS can be represented as a TWM in which the very small scattered intensity is amplified by beam coupling between the pump and scattered beam, the grating amplitude ν written in the following form is valid for both cases:

$$\nu = \frac{\pi \Delta n d}{\lambda \cos(\theta)}, \tag{6}$$

where Δn, d, λ, and θ are the refractive index change, the grating thickness, the incident wavelength, and the Bragg angle, respectively. The quantity ν depends on two main parameters at a certain wavelength and angle of incidence: the refractive index amplitude Δn and the grating thickness d. Due to the low value of modulation in HS, Δn for HS will be always much less than for TWM for the same thickness of the crystal. For a thick crystal, large ν increases the possibility to be in the dynamic regime due to the fact that the diffraction efficiency η is initially proportional to the square of the refractive index change by the relation $\eta = sin^2(\pi \Delta n d/\lambda \cos(\theta))$. For $\nu > \pi/2$ we have the so called overmodulation. We suppose that ν is a critical factor which can affect the values of activation energy. The situation is complicated as long as we are dealing with crystals of large thickness and refractive index change, i.e. for ν larger than one. This leads to problems that come from the absorption profile through the thickness of the crystal which should be well understood to ignore all these problems. A better approach would be to record for a short time to be always in the linear regime and to avoid the saturation effects of the sin^2 dependence of the diffraction efficiency on the refractive index change to be always in the kinematic recording range.[20]

To prove our assumption that overmodulation in TWM is a reason for the discrepancy in the values of activation energy determined by TWM and HS the temperature dependence of the compensation time constant needs to be investigated in a very thin crystal for which ν is expected to be much less than one using the different techniques.

There are some other reasons known in literature for the widely scattered values of the activation energy for protons migration or electron detrapping (0.9-1.4 eV). These may be due its dependence on the density of H^+ impurities, the oxidation state, the range of temperatures used in the experiment, the density of dopants[11,18,20,22–24] and the occurrence of different proton sites with different detrapping energies either OH^- substitution for O^{2-} ion or being an interstitial.[7] The high value of the activation energy for the iron doped crystal in comparison to the manganese doped crystal may be due to the migration of lithium self interstitials.[22,19]

In summary, three different techniques were used to measure the temperature dependence of the compensation time constant to evaluate the activation energy for thermal fixing. In comparison to the two holographic techniques

the DCC measurements were performed at a different temperature range which is a possible reason for the deviation in the values of the activation energy obtained from DCC and the other techniques.The discrepancy in the determined values of activation energy using HS and TWM may be due to two main reasons. The first reason is the possible dependence of the compensation time constant on the spatial frequency. At high concentration of free ions, it can be ignored and HS is expected to give the same results as TWM, whereas at low free ions concentration the it has to be taken into account. In TWM the dependence of compensation time constant on spatial frequency can be ignored only at high concentration of ions and low values of spatial frequency. On the other hand, as HS uses a multitude of **K**-vectors, not only one particular **K**-vector as in TWM, it is considered as an ideal technique to determine the concentraion of free ions if the spatial frequency dependence of the compensation time constant can be detected. The second reason is the difference in modulation depth in both techniques. HS is characterized by a very low modulation which assures being always out of the nonlinear regime that is possible with TWM. HS has some important advantages over the TWM, e.g., it is much simpler and does not need the high requirements for isolating vibrations in TWM.

ACKNOWLEDGMENTS

One of the authors (M. A. E.) is grateful for the financial support by ÖAD and the Egyptian government. This research was supported by the ÖAD-WTZ A-2/1998, and the OTKA Nos. T23092 and T26088.

REFERENCES

1. J. J. Amodei and D. L. Staebler, "Holographic pattern fixing in electro-optic crystals," *Appl. Phys. Lett.* **18**, pp. 540–2, 1971.
2. F. Chen, J. LaMachia, and D. Fraser, "Holographic storage in lithium niobate," *Appl. Phys. Lett.* **13**, pp. 223–5, 1968.
3. D. E. Staebler, W. J. Burke, W. Phillips, and J. J. Amodei, "Multiple storage and erasure of fixed holograms in Fe-doped $LiNbO_3$," *Appl. Phys. Lett.* **26**, pp. 182–4, 1975.
4. B. F. Williams, W. J. Burke, and D. L. Staebler, "Mobile Si ions in Fe-doped $LiNbO_3$ crystals. (fixing of thick-phase holograms)," *Appl. Phys. Lett.* **28**, pp. 224–6, 1976.
5. H. Vormann, G. Weber, S. Kapphan, and E. Krätzig, "Hydrogen as origin of thermal fixing in $LiNbO_3 : Fe$," *Solid State Commun.* **40**, pp. 543–5, 1981.
6. V. Kovalevich, L. Shuvalov, and T. Volk, "Spontaneous polarization reversal and photorefractive effect in single-domain iron-doped lithium niobate crystals," *Phys. Status Solidi (a)* **45**, pp. 249–52, 1978.
7. W. Bollmann and H. Stöhr, "Incorporation and mobility of OH^- ions in $LiNbO_3$ crystals," *Phys. Status Solidi (a)* **39**, pp. 477–84, 1977.
8. K. Buse, S. Breer, K. Peithmann, S. Kapphan, M. Gao, and E. Krätzig, "Origin of thermal fixing in photorefractive lithium niobate crystals," *Phys. Rev. B* **56**, p. 1225, 1997.
9. I. Nee, M. Müller, K. Buse, and E. Krätzig, "Role of iron in lithium-niobate crystals for the dark-storage time in holograms," *J. Appl. Phys.* **88**, pp. 4282–6, 2000.
10. Y. Yang, I. Nee, K. Buse, and D. Psaltis, "Ionic and electronic dark decay of holograms in $LiNbO_3 : Fe$ crystals," *Appl. Phys. Lett.* **78**, pp. 4076–8, 2001.
11. L. Arizmendi, P. Townsend, M. Carrascosa, J. Baquedano, and J. Cabrera, "Photorefractive fixing and related thermal effects in $LiNbO_3$," *J. Phys.: Condens. Matter* **3**, pp. 5399–06, 1991.
12. S. Klauer, M. Wöhlecke, and S. Kapphan, "Influence of H-D isotopic substitution on the protonic conductivity of $LiNbO_3$," *Phys. Rev. B* **45**, pp. 2786–99, 1992.
13. M. A. Ellabban, G. Mandula, M. Fally, R. A. Rupp, and L. Kovács, "Holographic scattering as a technique to determine the activation energy for thermal fixing in photorefractive materials," *Appl. Phys. Lett.* **78**(6), p. 844, 2001.
14. R. A. Rupp and F. W. Drees, "Light-induced scattering in photorefractive crystals," *Appl. Phys. B* **39**, pp. 223–229, 1986.
15. U. van Olfen, R. A. Rupp, E. Krätzig, and B. C. Grabmaier, "A simple method for the determination of the Li/Nb ratio of $LiNbO_3$ crystals," *Ferroel. Lett.* **10**, p. 133, 1989.
16. M. Fally, M. A. Ellabban, R. A. Rupp, M. Fink, J. Wolfsberger, and E. Tillmanns, "Characterization of parasitic gratings in $LiNbO_3$," *Phys. Rev. B* **61**, p. 15778, 2000.

17. M. A. Ellabban, R. A. Rupp, and M. Fally, "Reconstruction of parasitic holograms to characterize photorefractive materials," *Appl. Phys. B* **72**, pp. 1–6, 2001.
18. M. Carrascosa and L. Arizmendi, "High-temperature photorefractive effects in $LiNbO_3 : Fe$," *J. Appl. Phys.* **73**, pp. 2709–13, 1992.
19. I. Nee, K. Buse, F. Havermeyer, R. A. Rupp, M. Fally, and R. P. May, "Neutron diffraction from thermally fixed gratings in photorefractive lithium niobate crystals," *Phys. Rev. B* **60**, p. R 9896, 1999.
20. A. Yariv, S. S. Orlov, and G. A. Rakuljic, "Holographic storage dynamics in lithium niobate: Theory and experiment," *J. Opt. Soc. Am. B* **13**, pp. 2513–23, 1996.
21. R. Müller, L. Arizmendi, M. Carrascosa, and J. M. Cabrera, "Determination of H concentration in $LiNbO_3$ by photorefractive fixing," *Appl. Phys. Lett.* **60**, pp. 3212–4, 1992.
22. D. H. Jundt, M. M. Fejer, R. G. Norwood, and P. F. Bordui, "Composition dependence of lithium diffusivity in lithium niobate at high temperature," *J. Appl. Phys.* **72**, pp. 3468–73, 1992.
23. R. Müller, L. Arizmendi, M. Carrascosa, and J. Cabrera, "Time evolution of photorefractive fixing processes in $LiNbO_3$," *Opt. Mat.* **4**, p. 2909, 1995.
24. L. Kovács and K. Polgár, "Conductivity of lithium niobate," in *Properties of Lithium Niobate*, INSPEC London and New York, ed., pp. 109–14, EMIS Datareviews Series No. 5., 1989.